Charge and Spin Order in La$_{2-x}$Sr$_x$NiO$_4$ (x=0.275 and 1/3)

S.-H. Lee[1,2], S-W. Cheong[3], K. Yamada[4], and C.F. Majkrzak[1]

[1]*NIST Center for Neutron Research, National Institute of Standards and Technology, Gaithersburg, MD 20899*
[2]*University of Maryland, College Park, Maryland 20742*
[3]*Department of Physics and Astronomy, Rutgers University and Bell Laboratories, Lucent Technologies, Murray Hill, NJ 07974*
[4]*Kyoto University, Institute of Chemical Research, Uji 611-0011, Kyoto, Japan*

We report polarized and unpolarized neutron diffraction measurements on La$_{2-x}$Sr$_x$NiO$_4$ (x=0.275 and 1/3). The data for the spin ordered states are consistent with a collinear spin model in which spins with S=1 are in the NiO$_2$ plane and are uniformly rotated from the charge and spin stripe direction. The deviation angle is larger for x=1/3 than for x=0.275. Furthermore, for x=1/3 the ordered spins reorient below 50 K, which suggests a further lock-in of the doped holes and their magnetic interactions with the S=1 spins.

PACS numbers: 75.30.Fv, 71.45.Lr, 75.25.+z, 74.72.-h

Since the discovery of incommensurate (IC) magnetic fluctuations in superconducting cuprates [1], magnetism in doped antiferromagnets has attracted much attention. Doping holes into the antiferromagnetic (AFM) insulator La$_2$CuO$_4$ rapidly weakens the static magnetic correlations and leads to a metallic, superconducting phase at moderate hole concentrations [2]. The discovery of static IC spin and charge peaks in La$_{1.6-x}$Nd$_{0.4}$Sr$_x$CuO$_4$ [3] led to a model of charge stripes acting as antiphase domain walls for the intervening AFM regions [3,4].

La$_2$NiO$_4$ is a Mott insulator with $T_N \simeq 650$ K and spins aligned with the shortest orthorhombic lattice direction [5]. Doping of divalent Sr^{2+} ions into the trivalent La^{3+} sites in La$_{2-x}$Sr$_x$NiO$_4$ (LSNO(x)) rapidly suppresses the ordering but the compound remains insulating until $x \approx 1$ where it becomes metallic. For $x > 0.1$, IC charge and spin superlattice reflections appear, and can be characterized by $Q_{spin} = (1 \pm \epsilon, 0, 0)$ and $Q_{charge} = (2\epsilon, 0, 1)$ with $\epsilon \approx x$ [6–9]. For $x \approx 1/3$, there is a commensurability effect which favors $\epsilon = 1/3$ [9].

Considering that the static spin structure should be a basis for understanding the nature of spin and charge stripes in the doped nickelates and cuprates, it is surprising that the local spin structure, evolving upon doping, has not been studied. In this letter we report polarized and unpolarized neutron diffraction measurements on LSNO(x=0.275 and x=1/3) and present a collinear spin model to explain our data in which spins are rotated uniformly by an angle θ from the stripe direction. For x=0.275, the angle θ is 27(7)^o below $T_N = 155(5)$ K. For x=1/3, $\theta = 40(3)^o$ for 50 K $< T < T_N = 200(10)$ K and below 50 K another phase transition occurs involving reorientation of spins to $\theta = 53(3)^o$. We argue that the spin reorientation is due to a further localization of the doped holes on the lattice, which is consistent with recent resistivity measurements that showed a delocalization of charge stripes by an electic field (although in the lowest temperature phase the charge stripes are more robust.) [10] Our polarized neutron data also provide unequivocal

evidence that upon cooling the charge order precedes the spin order in these materials. Charge orders at 200(10) K for x=0.275, and at 240(10) K for x=1/3.

The LSNO(x) crystals with x=0.275 and x=1/3 used in this work were grown by the floating-zone method at Kyoto University and at Bell Laboratories, respectively. The crystal structure of both materials remains tetragonal with the I4/mmm symmetry over the range of temperature, 10 K $< T <$ 320 K, with $a_t = 3.82(1)$ Å and $c = 12.64(5)$ Å at 11 K for x=0.275 and with $a_t = 3.83(1)$ Å and $c = 12.69(5)$ Å at 11 K for x=1/3. For convenience, however, we use orthorhombic lattice units with $a_o = \sqrt{2}a_t$ which is rotated by 45° with respect to the Ni-O bonds in the NiO$_2$ planes.

Neutron scattering measurements were performed on the cold neutron triple axis spectrometer SPINS at NIST. The incident neutron energy was $E_i = 5$ meV and higher order contamination was eliminated by a cryostat-cooled Be filter before the sample. The incident neutrons were polarized in one spin state by a forward transmission polarizer. The spin state of the scattered neutrons from the sample was then analyzed with a rear flipper and polarizer combination. A collimator was placed right after each polarizer to eliminate the other spin state. The samples were mounted in such a way that the (h0l) reciprocal plane becomes the scattering plane. A guide field was applied vertically along the (010)-axis. Collimations were guide-40-40-open for the LSNO(x=0.275) measurements and guide-40-20-open for the LSNO(x=1/3) measurements. The polarizing efficiency was 0.89(1) for the former and 0.90(1) for the latter. In this geometry, the spin component perpendicular to the wavevector transfer $\vec{Q}$ which is parallel with the guide field together with the nuclear structural component, contribute to non-spin-flip (NSF) channel whereas the spin component normal to $\vec{Q}$ and to the guide field contributes to the spin-flip (SF) channel. Since spins in the nickelates are coplanar in ab-plane [5,11], the NSF and SF neutron scattering cross sections for $Q = (h0l)$, $\sigma_{NSF}(Q)$ and $\sigma_{SF}(Q)$ respectively, can be written as [12]

$$\sigma_{NSF}(Q) = \sigma_N(Q) + \sigma_M^b(Q)$$

$$\sigma_{SF}(Q) = \sigma_M^a(Q) \left(1 - \frac{(ha^*)^2}{(ha^*)^2 + (lc^*)^2}\right) \qquad (1)$$

where σ_N is the structural scattering cross section, σ_M^a and σ_M^b are the a- and b-component of the magnetic scattering cross section, respectively.
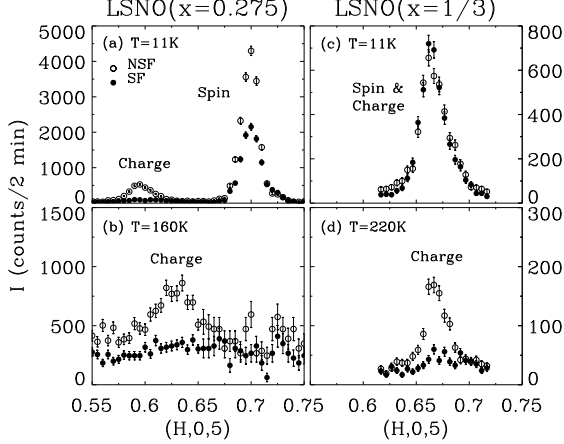

Fig. 1. Polarized elastic neutron scattering data along (h05) from LSNO(x=0.275) ((a) and (b)), and from LSNO(x=1/3) ((c) and (d)).

Fig. 1 shows the results of polarized neutron diffraction on LSNO(x=0.275 and 1/3). For x=0.275, at 11K the data exhibit two types of superlattice peaks: the first harmonic at (0.7,0,5) separated by $(\epsilon, 0, 0)$ from the (105) AFM Bragg reflection in pure La_2NiO_4 and the second harmonic at (0.6,0,5) separated by $(2\epsilon, 0, 1)$ from the (004) nuclear Bragg reflection with $\epsilon = 0.3 \approx x$ [9]. The first harmonic has both NSF and SF components whereas the second harmonic has a NSF component only. These provide direct and unambiguous evidence that the first harmonic is magnetic (spin peak) whereas the second harmonic is non-magnetic (charge peak) in origin, and suggest the formation of charge stripes acting as AFM domain walls (see Fig. 2). As shown in Fig. 3 (a), the charge peak gradually increases below T_c and then get enhanced in a weakly first order at T_s when spins order. Inplane charge correlation length, ξ_c, also increases at T_s. In the charge and spin ordered phase the charge peak is broader than the spin peak, indicating that ξ_c is shorter than inplane spin correlation length, ξ_s: $\xi_c/\xi_s \approx 100$ Å/300 Å = 1/3 (see the inset of Fig. 3 (a)). It has been argued [13] that disorders in the stripes are mostly due to non-topological elastic deformations along the stripes and the decrease of the correlation lengths is inversely proportional to a power of the periodicity, which can explain why ξ_c is smaller than ξ_s even though the charge and spin correlations are inexorably connected. For comparison, $\xi_c/\xi_s = 1/4$ for $La_{1.6-x}Nd_{0.4}Sr_xCuO_4$ [14]. As shown in Fig. 1 (a) and (b), upon heating the (0.7,0,5)

and (0.6,0,5) superlattice peaks shift toward $(\frac{2}{3}, 0, 5)$ until the (0.7,0,5) peak vanishes at 155(5) K and the (0.6,0,5) peak at 200(10) K. In the intermediate temperature range $(155K < T < 200K)$, as shown in Fig. 1 (b), the charge order exists without the spin order. For x=1/3, at 11 K the first and second harmonics with $\epsilon = x$ come together at the same wave vector as shown in Fig. 1 (c). Unlike the case for x=0.275, the position of the superlattice peak for x=1/3 is independent of T, implying the stability of commensurability [15]. At 220 K, the (2/3,0,5) peak has a NSF component only, indicating that the x=1/3 system also has an intermediate T phase with charge order only.
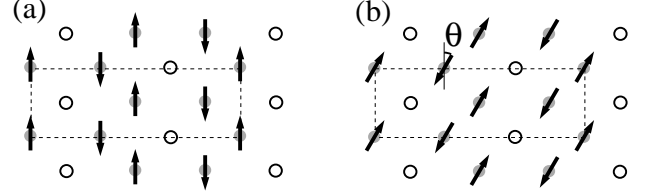

Fig. 2. Possible spin structures in a NiO_2 plane for LSNO(x=1/3). (a) Spins are perpendicular to the propagation vector along the (100)-axis. (b) Spins are uniformly rotated by an angle θ from the (010)-axis. Dashed lines indicate the magnetic unit cell.

Besides identifying the origins of the scattering, polarized neutron diffraction data also allow us to determine the spin structure in the material. Firstly, it is to be noted that the spin peaks in the spin ordered states of both samples are SF in nature. If spins are aligned along the (010)-direction (see Fig. 2 (a)), $\sigma_M^a = 0$ and Eq. (1) would yield zero SF scattering. There are two possible scenarios to produce nonzero SF scattering. One possibility is two magnetic domains with a propagation vector along (100)-axis: in one domain spins are perpendicular to and in the other parallel to the propagation vector. The population of the domains must be unequal to explain our data, which seems unlikely. The other possibility is one single magnetic domain with $\sigma_M^a \neq 0$.

For quantitative studies of the spin structure, we have studied the T-dependence of the NSF and SF scattering at various superlattice reflections from both samples. Fig. 3 (b) shows some of the results for x=1/3. Upon cooling at 240 K NSF scattering at the (2/3,0,5) reflection develops without SF scattering, indicating charge ordering. Below around 200 K, SF as well as NSF scattering increases due to spin ordering in the usual second order fashion. At 50 K, however, the trend changes: the NSF scattering decreases whereas the SF increases. This behavior can be more clearly seen in the ratio of SF to NSF scattering shown in Fig. 3 (c). The sharp increase in the ratios below 50K indicates that the phase transition at 50 K involves reorientation of spins. For x=0.275, the SF to NSF ratios of the spin peak in the spin-ordered

phase were smaller than those for the corresponding reflections in the x=1/3 system and no spin reorientation transition was observed down to 10K.
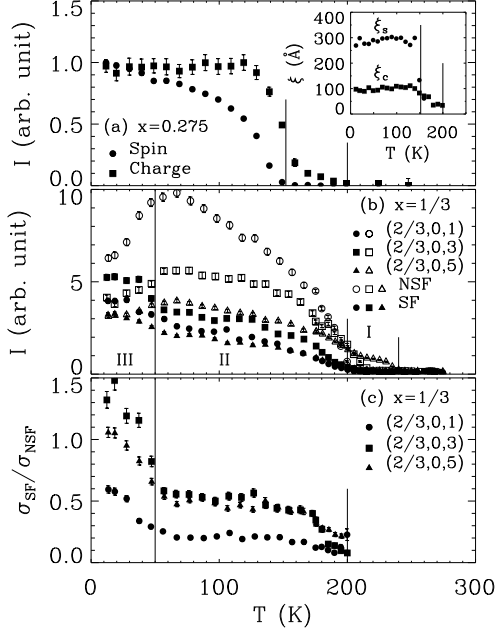

Fig. 3. (a) T-dependence of unpolarized elastic neutron scattering intensities of the charge peak and the spin peak. (b) NSF (open symbols) and SF (filled symbols) scattering intensities at various superlattice reflections from LSNO(x=1/3) as a function of T. (c) T-dependence of the ratio of SF to NSF scattering intensities after backgrounds were determined above the transition temperature and subtracted. Correction for finite polarizing efficiency was also made [16].

The symbols in Fig. 4 summarize the measured σ_{SF}/σ_{NSF} for LSNO(x=0.275) and for the two spin-ordered phases in LSNO(x=1/3). The data show a general trend: for a given value of h in each phase, σ_{SF}/σ_{NSF} increases as l increases with an exception at the $(2/3,0,5)$ reflection for x=1/3. The deviation of the $(2/3,0,5)$ reflection is due to the fact that the $(2/3,0,5)$ peak has a charge component as well as spin component. Our unpolarized neutron scattering data along $(0.6, 0, 0 \leq l \leq 5)$ on the x=0.275 sample have the strongest intensity at $l = 5$ but negligible at other l, indicating the structure factor due to charge ordering is strong at $(0.6, 0, 5)$ but not at other l. We expect the same holds for x=1/3.

Now consider the collinear spin structure shown in Fig. 2 (b) in which spins are rotated by θ about the c-axis. Since the spins have a b-component, SF scattering would be non-zero and the ratio of SF to NSF scattering would be determined by the angle θ. The lines in Fig. 4 are the calculated σ_{SF}/σ_{NSF} for the spin structure shown in Fig. 2 (b):

$$\frac{\sigma_{SF}}{\sigma_{NSF}} = \tan^2\theta \cdot \left(1 - \frac{(ha^*)^2}{(ha^*)^2 + (lc^*)^2}\right). \qquad (2)$$
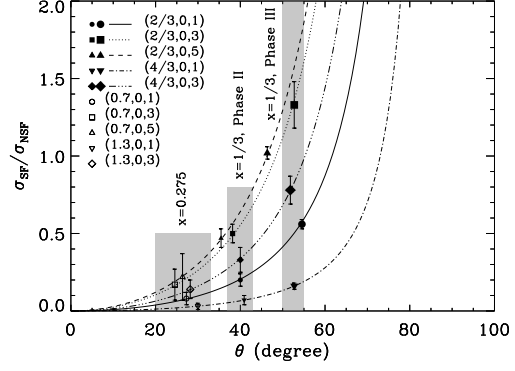

Fig. 4. Experimental (symbols) and the model calculated (lines) ratios of SF to NSF scattering cross sections as a function of the rotation angle θ.

From the comparison to the data, we conclude that $\theta = 27^o \pm 7^o$ for x=0.275, $40^o \pm 3^o$ for phase II and $52.5^o \pm 2.5^o$ for phase III in the x=1/3 sample. We can also estimate the charge contribution in the $(2/3,0,5)$ reflection to be $\frac{\sigma_N}{\sigma_M^b} = 0.20(6)$. For x=0.275 (see Fig. 1(a)) $\frac{\sigma_N}{\sigma_M^b} = \frac{\sigma_{NSF}(0.6,0,5)}{\sigma_{NSF}(0.7,0,5)} = 0.12(1)$.

Unpolarized neutron diffraction data along the l-direction also contain information on spin structure. As shown in Fig. 5, the peaks are much sharper in l for x=0.275 than for x=1/3, which indicates that the correlations in x=0.275 are nearly three-dimensional whereas those in x=1/3 are quasi-two-dimensional. Another obvious difference between them is that the even l to old l peak intensity ratio, $\frac{I(even\ l)}{I(odd\ l)}$, is much larger for x=0.275 than for x=1/3. There are other subtle features to be noted. For x=0.275, the odd l peak weakens as l increases whereas the even l peak is strongest at $l = 2$. For x=1/3, at 180K (phase II) the odd l peak also weakens as l increases. However at 15K (phase III) the $l = 3$ peak becomes strongest. If the spin structure of Fig. 2 (a) is displaced by $(\frac{a}{2}n, \frac{1}{2}, \frac{1}{2})$ in neighboring NiO_2 planes, the magnetic neutron scattering cross section would become $\sigma(Q) \propto |F(Q)|^2(1 + (-)^l\cos n\pi h)$ [17] where F is the magnetic form factor of the Ni^{2+}. Therefore, for a given h, the l-dependence of odd or even l peaks would just follow $|F(Q)|^2$. This $\sigma(Q)$ cannot explain those subtle features. On the other hand, the spin structure of Fig. 2 (b) would give

$$\sigma(Q) \propto |F(Q)|^2(1 + (-)^l\cos n\pi h)$$
$$\times \left(1 - \sin^2\theta\frac{(ha^*)^2}{(ha^*)^2 + (lc^*)^2}\right). \qquad (3)$$

With the θ's which are obtained from the polarization analysis, Eq. 3 reproduces the l-dependence remarkably well for the case of x=0.275 with three-dimensional magnetic correlations, as shown as shaded bars in Fig. 5.
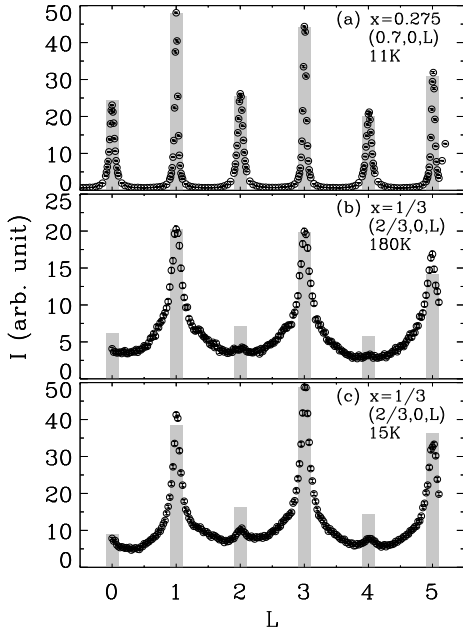
3

Fig. 5. l-dependence of (a) (0.7,0,l) scan form LSNO(x=0.275) at 11 K, and (2/3,0,l) scan from LSNO(x=1/3) (b) at 180 K and (c) 15 K. The shaded bars are obtained by the model which is described in the text.

In the case of x=1/3 where the magnetic order is quasi-two dimensional, the long tails of the peaks make it difficult to extract the integrated intensities to compare with the model. Nevertheless, the model explains the subtle features such as the (2/3,0,3) peak being considerably stronger than the other reflections in phase III.

Spin reorientations upon cooling have been observed in some isostructural materials such as pure La_2CoO_4 [18] and Nd_2CuO_4 [19]. Those reorientations involve spin flip (by $\pi/2$ or π) which are due to either a structural phase transition (in La_2CoO_4) or strong coupling between the rare-earth moments and Cu^{2+} moments (in Nd_2CuO_4). For LSNO(x=1/3), however, there is no structural phase transition down to 10 K within our experimental uncertainty [20]. What causes then the reorientation of spins in LSNO(x=1/3) below 50 K ? The answer might be a further localization of the holes on the lattice and their interactions with the surrounding S=1 Ni^{2+} moments. Among the two charge ordered states, below and above 50 K, the holes should be more strongly pinned on the lattice in the lower T phase. The further localization of the holes might either induce a subtle and yet undetected local crystal distortion around the surrounding S=1 spins or magnetically order themselves, either of which would in turn reorient the S=1 spins. This idea is consistent with recent resistivity measurements [10]. In the resis-tivity measurements, a moderate inplane electric field ($V_{cir} \geq 100$ V) decreases the resistivity by up to 5 orders of magnitude in phase II. However, although the charge-ordered state in phase III becomes suppressed by the electric field, phase III survives until $V_{cir} \geq 900$ V, which indicates the stronger localization of the holes in phase III than in phase II. Understanding the microscopic origin of the further localization in LSNO(x=1/3) and its effects, such as the spin reorientation, as well as the evolution of spin structure upon doping in LSNO(x) requires more theoretical and experimental studies.

[1] S-W. Cheong *et al.*, Phys. Rev. Lett. **67**, 1791 (1991).
[2] K. Yamada *et al.*, Phys. Rev. B **57**, 6165 (1998).
[3] J.M. Tranquada *et al.*, Nature **375**, 561 (1995); Phys. Rev. Lett. **78**, 338 (1997).
[4] V. J. Emery, S. A. Kivelson, and J. M. Tranquada, Proc. Natl. Acad. Sci. **96**, 8814 (1999) and references therein.
[5] G. Aeppli and D.J. Buttrey, Phys. Rev. Lett. **61**, 203 (1988).
[6] S.M. Hayden *et al.*, Phys. Rev. Lett. **68**, 1061 (1992).
[7] C.H. Chen, S-W. Cheong and A.S. Cooper, Phys. Rev. Lett. **71**, 2461 (1993).
[8] J.M. Tranquada *et al.*, Phys. Rev. Lett. **73**, 1003 (1994); Phys. Rev. B **52**, 3581 (1995); Phys. Rev. B **54**, 12318 (1996).
[9] H. Yoshizawa, *et al.*, cond-mat/9904357.
[10] S. Yamanouchi *et al.*, Phys. Rev. Lett. **83**, 5555 (1999).
[11] Our polarized neutron diffraction measurements on the LSNO(x=1/3) sample in the (hk0) scattering plane confirmed that the spins lie in the ab-plane.
[12] R.M. Moon *et al.*, Phys. Rev. **181**, 920 (1969).
[13] O. Zachar, cond-mat/9911171.
[14] J.M. Tranquada *et al.*, Phys. Rev. B **59**, 14712 (1999).
[15] S.-H. Lee and S-W. Cheong, Phys. Rev. Lett. **79**, 2514 (1997).
[16] C.F. Majkrzak, Physica B **221**, 342 (1996).
[17] P. Wochner *et al.*, Phys. Rev. B **57**, 1066 (1998).
[18] K. Yamada *et al.*, Phys. Rev. B **39**, 2336 (1989).
[19] S. Skanthakumar *et al.*, Physica C **160**, 124 (1989).
[20] Neither a splitting of the lattice constant a (orthorhombic distortion) nor a superlattice reflection at (102) (allowed for another tetragonal P4$_2$/ncm structure) has been found in LSNO(x=1/3) for 10 K $< T <$ 320 K.